assumption that solute addition tends to break up the structure of the solvent through reactions such as

$$(HNO_3)_{a+b} + (a/2)\ NO_3^- \rightarrow (a/2)\ NO_3^- \cdot (HNO_3)_2 + b\ HNO_3 \quad (8)$$

leading to a net decrease in volume. One might expect a further weakening of the solvent structure if the addition of solute lowers the dielectric constant of the solution. At low solute concentration, reactions such as Equation 8 will facilitate the formation of ion-solvent complexes on further addition of solute and lead to a decrease in $\bar{v}_2$ with concentration. At high concentrations, there will be the more usual increase in $\bar{v}_2$ with molality as the concentration of solvent molecules available for ion-solvent association decreases, and repulsion between ions becomes more important. Results similar to the minima near 1 molal had been previously reported by Klemenc and Rupp (*4*) for the HNO_3-NO_2 system and, more recently, by Potier and Potier (*7*) for HNO_3-KNO_3 solutions.

LITERATURE CITED

(1) Antipenko, G.L., Beletskaya, E.S., Korleva, Z.I., *Zhur. Priklad. Khim.* **32**, 1462 (1959).
(2) Antipenko, G.L., Beletskaya, E.S., Krylova, A.G., *Ibid.*, **31**, 847 (1958).
(3) Chedin, J., Vandoni; R., *Compt. rend.* **227**, 1232 (1948).
(4) Klemenc, V.A., Rupp, J., *Z. anorg. u. allgem. Chem.* **194**, 51 (1930).
(5) Klotz, I.M., "Chemical Thermodynamics," p. 203, Prentice-Hall, New York, 1950.
(6) Mason, D.M., Petker, I., Vango, S.P., *J. Phys. Chem.* **59**, 511 (1955).
(7) Potier, A., Potier, J., *Bull. soc. chim. France* **1958**, 439.
(8) Robinson, R.A., Stokes, R.H., "Electrolyte Solutions," p. 367, Butterworths Scientific Publ., London, 1955.
(9) Schulz, Gerhard, *Z. physik. Chem.* **B40**, 151 (1938).
(10) Stern, S.A., Kay, W.B., *J. Am. Chem. Soc.* **76**, 5353 (1954).

RECEIVED for review March 13, 1961. Accepted June 28, 1961.

Porous Structure of Catalyst Materials

R. M. DeBAUN, S. F. ADLER, and R. D. FINK[1]
American Cyanamid Co., Stamford, Conn.

THE POROUS STRUCTURE of catalyst materials and of catalyst supports has received continuous attention for some years. In the proceedings of a recent conference on porous materials (*8*), interest in catalyst materials as porous bodies was made evident. In another review (*14*), the relevance of the porous structure of the catalyst not only to catalyst activity but also to catalyst selectivity was developed extensively.

To study porous structure in greater detail, various schemes have been developed whereby the adsorption and/or desorption isotherms can be translated into "pore size distributions." In the one case (*4, 6*), sorption data are interpreted as describing the lengths associated with straight-sided cylindrical pores of a given size. In this way, the data can also be related to the area (or the volume) associated with pores of radius up to and including a certain size. In the other case (*7, 11, 13*), the sorption data are related to a physical model which represents a pore as a slit between two flat parallel plates.

The physical model is, no doubt, strictly correct in neither case. In fact, an exhaustive study of any particular porous body would almost certainly require both adsorption and desorption measurements, mercury porosimeter measurements (*12*), etc. For example, as shown by deBoer and Everett (*8*), the "shape" of the whole isotherm, including the hysteresis loop, can tell a good deal about what kind of geometry can be attributed to the pore structure—viz., "blind" pores, tapered pores, "bottle"-shaped pores, and others. Indeed, in using diffusion measurements to study porous structure, useful information may be obtained (*3*) by distinguishing between steady-state and transient measurements.

On the other hand, comparison (especially within a series of chemically similar materials) of pore size distributions as calculated by some consistent scheme will in many cases lead to fruitful distinctions between catalyst materials. Such might arise, for example, in studies on catalyst development, where it is desirable to distinguish among a series of catalyst preparations in order to follow the effect of variations in preparation technique. Alternatively, such considerations might be useful in assisting catalyst users (such as refiners) in selecting the most suitable catalyst grade from a line of available catalysts.

In this report, we describe, in summary form, an examination of the pore size distributions of a series of catalyst materials either actually or potentially usable in oil refining processes. In all cases shown, the distributions can be approximated by a single relatively simple model; moreover, the distributions can be reproduced by simple measurements which are normally made on most catalyst samples—namely, the total pore volume and the B.E.T. surface area.

EXPERIMENTAL

Samples. Preparations studied were mainly samples of commercial or commercial-type cracking, reforming, or hydrodesulfurization catalysts. Some of the samples were pilot plant preparations; one group (4 to 8) was provided by Koninklijke Zwavelzuurfabrieken v/h Ketjen n.v. of

[1] Present address, Department of Chemistry, Massachusetts Institute of Technology, Cambridge, Mass.

Amsterdam, Holland. All samples were given a preliminary treatment at 1100° F. for 1 hour prior to examination. The samples studied cover broad ranges of the processing variables appropriate to their particular manufacture—for example, the influence of processing techniques on cracking catalysts manufacture has been discussed by Ashley and Innes (2).

Sorption Data. Surface area measurements, nitrogen pore volumes, and nitrogen adsorption isotherms were obtained for most materials by previously reported techniques (*1, 9, 10*). The samples provided by Ketjen were studied by them using similar methods. Adsorption and desorption data are tabulated using values from smoothed curves. In most cases only adsorption data are shown, although desorption data are given for a few samples. The surface area shown is obtained by Relation 1

$$\text{Area} = 3.68\ V_{0.2} \qquad (1)$$

where $V_{0.2}$ is the volume of nitrogen in standard cubic centimeters sorbed at a relative pressure of 0.2. This relation is obtained by substituting $p/p_0 = 0.2$ into the B.E.T. equation (*5*), using 16.2 sq. A. per mole for the nitrogen area and assuming a C value of 70. This "abbreviated" B.E.T. determination gives results in reasonably good agreement with the rigorous B.E.T. determination for materials of the type included here. Accordingly, the area figure also gives the value of the isotherm at $p/p_0 = 0.2$.

Water pore volumes were obtained on formed material by first crushing the pellets or extrudates to a fine powder and then measuring the water sorbed by these particles. Thus the pore volumes shown should represent only the microporosity, inasmuch as crushing formed material to a fine powder removes interparticle void spaces (> 250 A.) which represent large pores between the granules.

Analysis. Pore size distributions were calculated using a parallel plate model (*11*). The pore size distributions for both volume and area are also tabulated.

Experimental Results. The experimental data are listed in Table I. On plotting the area and volume distributions in various ways, it was found that all the area distributions could be approximated by a logarithmic normal form. Figure 1 shows the pore size distributions for typical cracking catalysts. Figure 2 shows the pore size distributions of a typical alumina used in preparing hydrodesulfurization catalyst and an alumina-based catalyst which fits the model relatively poorly as compared to the other materials studied. Even in this case, the model of a logarithmic normal pore size distribution was a good approximation in the central region (5 to 95%) of the pore size distribution.

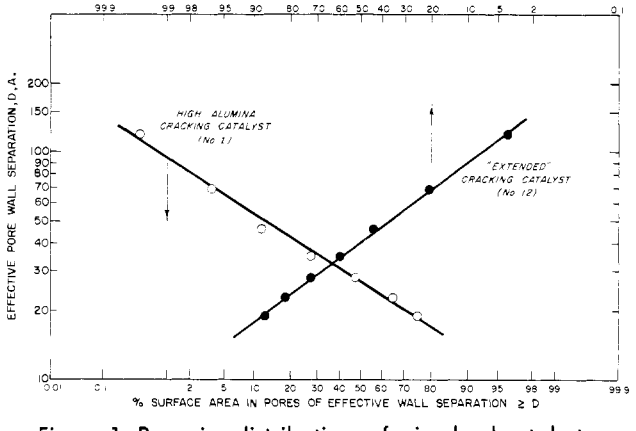

Figure 1. Pore size distributions of mixed gel catalysts

In view of the relatively good approximation to the logarithmic normal model of the distribution of areas, we have been able to summarize these distributions by two parameters. P_{50} is the value of pore wall separation in Angstrom units corresponding to 50% of the surface area and P_{25}/P_{75} is the ratio of the pore wall separations corresponding to 25 and 75%, respectively, of the surface area. These correspond then to measures of the location and the spread of the pore distribution.

In some materials, notably the alumina-based samples (Nos. 14 to 31), the area (or volume) is used up in the numerical solution before the full spectrum of pore sizes is finished. This is attributed by deBoer (*8*) to bottle-shaped pores, to pores with intermittent constrictions, or to pore intersections which effectively produce additional porosity without corresponding pore wall area.

The fact that such effects are relatively small—namely, that the B.E.T. area is well accounted for by the area calculated from the pore size distribution—indicates that, in general, the pore systems of these materials behave like independent domains and that pores with wide bodies and very narrow necks seem relatively infrequent.

In general, cracking catalyst materials (Nos. 1 to 13) have appeared to fit the suggested logarithmic normal model slightly better than alumina or alumina-based materials (Nos. 18 to 31). However, even the latter are fairly well approximated by such a model. In general, cracking catalyst materials show a higher relative spread parameter (average $P_{25}/P_{75} = 2.77$ for Nos. 1 to 13 *vs.* 1.95 for Nos. 18 to 31). This is connected with a somewhat lower "mean" value for the cracking catalysts (average $P_{50} = 25.6$ for Nos. 1 to 13 *vs.* 46.2 for Nos. 14 to 31).

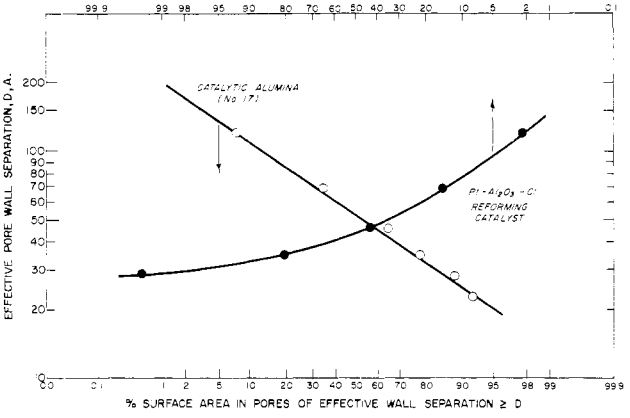

Figure 2. Pore size distributions of alumina-base catalysts

Inasmuch as all the distributions seem to be characterizable by members of the two-parameter distribution family (the log normal distribution), it is tempting to believe that the entire distribution of pore sizes can be predicted from any two independent facts about the pore structure of the sample. Two which immediately come to mind are the surface area and pore volume of the sample. Indeed, in the theory presented by Wheeler (*14*), the mean pore diameter is said to be proportional to the ratio of pore volume and surface area. Accordingly, we attempted to predict these pore characters by a model such as 2a to 2d.

$$\log (P_{50}) = a_0 + a_1 \log (10\ V) + a_2 \log A/100 \qquad (2a)$$

$$\log (P_{25}/P_{75}) = b_0 + b_1 \log (10\ V) + b_2 \log A/100 \qquad (2b)$$

$$3\ a_1 + 2\ a_2 = 1 \qquad (2c)$$

$$3\ b_1 + 2\ b_2 = 0 \qquad (2d)$$

where

V = pore volume, cc. per gram
A = surface area, in sq. meters per gram

Table I. Sorption Characteristics of Catalyst Samples[a]

No.	Catalyst Type	Isotherm, Sorption V/V_0 at P/P_0 = 0.3	0.4	0.6	0.8	Pore Volume, Cc./G. H_2O	N_2	Surface Area, Sq. M^2/G.	Pore Size Distribution, Area: % Area in Pores > D, A. 120	69	46	35	28	23	19	P_{50}	P_{25}/P_{75}	Pore Size Distribution, Volume (% Pore Volume in Pores > D, A.) 120	69	46	35	28	23	19
												Synthetic Cracking Catalyst														
	25% Al_2O_3	0.35	0.42	0.65	0.90	0.63	0.63	445	0.4	3.6	11.5	27.6	47.2	64.7	74.9	27.5	1.90	3.6	13.2	28.5	50.5	71.4	86.6	94.5
2	25% Al_2O_3	0.38	0.45	0.60	0.84	0.67	0.65	522	0.8	4.3	12.4	24.6	35.9	45.1	56.5	21.5	2.48	7.5	19.4	36.6	55.1	68.4	77.1	86.6
3	13% Al_2O_3	0.42	0.49	0.66	0.88	0.70	0.69	609	0.5	3.2	9.4	19.3	29.8	41.7	53.6	20.0	2.40	5.5	15.6	30.2	47.0	60.9	74.5	84.4
4	13% Al_2O_3	0.73	0.82	0.97	1.00	0.40	0.40	588	0.0	0.0	0.2	1.5	6.6	15.8	27.6	15.0	1.78	0.0	0.0	0.7	4.5	15.8	32.1	50.0
		[b] 0.73	0.83	0.99	1.00				0.0	0.0	0.2	0.5	2.6	17.7	30.4			0.0	0.0	0.7	1.6	6.4	33.1	52.3
5	13% Al_2O_3	0.43	0.51	0.73	0.96	0.61	0.61	518	0.1	1.1	6.5	20.6	37.0	49.7	63.2	23.0	2.00	1.3	5.0	17.5	40.6	61.7	74.9	86.9
		[b] 0.43	0.51	0.92	0.98				0.05	0.6	1.8	5.8	43.8	61.5	73.1			0.5	2.5	5.4	11.8	60.7	81.0	91.7
6	13% Al_2O_3	0.32	0.37	0.57	0.94	0.75	0.75	485	0.04	2.7	21.3	40.2	59.3	68.7	75.9	31.5	2.23	0.3	7.8	40.4	64.2	83.0	90.5	95.7
		[b] 0.32	0.37	0.70	0.96				0.04	1.6	3.5	35.8	75.9	90.1	94.8			0.3	4.6	8.0	48.4	87.4	87.8	
7	13% Al_2O_3	0.25	0.28	0.38	0.66	0.91	0.91	452	0.8	19.7	37.8	49.9	59.0	63.2	68.7	34.0	4.13	5.0	45.3	69.9	81.7	88.6	91.4	94.5
		[b] 0.25	0.28	0.41	0.88				0.0	7.4	45.0	62.2	77.7	79.2	82.1			0.0	15.7	66.7	83.4	95.1	96.3	98.2
8	13% Al_2O_3	0.41	0.48	0.71	0.99	0.61	0.61	495	0.02	0.2	6.9	25.9	43.7	56.9	68.4	26.0	2.12	0.2	0.8	15.6	45.5	66.3	80.4	90.4
		[b] 0.42	0.52	0.91	0.99				0.02	0.2	2.3	7.9	31.1	73.9	91.6			0.2	0.8	5.6	14.3	42.6	84.7	99.9
9	25% MgO	0.59	0.67	0.88	0.97	0.48	0.48	568	0.1	0.5	2.1	6.2	15.4	29.2	40.2	16.5	2.21	1.7	3.7	8.9	18.2	34.7	54.6	68.1
10	25% MgO	0.40	0.45	0.63	0.86	0.63	0.73	615	0.7	3.7	11.3	21.4	32.9	44.6	51.8	21.0	2.40	7.1	16.1	34.2	51.6	66.1	78.1	84.7
												Partially Synthetic Cracking Catalyst														
11		0.23	0.28	0.40	0.70	0.52	0.51	252	2.0	14.6	34.0	51.5	62.6	71.2	79.8	35.5	2.50	12.0	38.1	63.7	80.3	88.3	93.7	98.3
12		0.20	0.23	0.34	0.62	0.72	0.70	282	4.0	20.5	44.3	60.0	72.6	81.8	87.5	41.5	2.45	19.2	47.0	72.6	84.7	92.3	96.8	99.4
13		0.29	0.32	0.46	0.67	0.56	0.71	459	2.8	9.1	18.2	28.0	41.0	49.3	51.0	20.5	3.45	22.0	39.6	55.8	68.2	81.0	87.7	89.2
												Fluid Reforming Catalyst														
14	10% MoO_3	0.39	0.46	0.62	0.79	0.31	0.30	276	1.4	4.0	9.4	15.8	24.6	35.8	46.9	18.0	2.42	15.4	25.4	38.5	49.7	61.5	73.6	84.0
												Hydrodesulfurization Catalyst														
15	15% MoO_3 3% CoO	0.24	0.29	0.44	0.68	0.50	0.48	235	3.2	13.1	27.0	45.1	61.9	76.0	86.3	32.0	2.13	18.4	38.6	56.5	73.2	85.3	93.5	98.9
16	15% MoO_3 3% CoO	0.22	0.27	0.39	0.65	0.65	0.62	239	4.6	18.7	38.7	61.2	76.5	90.3		40.0	2.04	20.8	42.8	62.8	78.9	87.5	93.7	
												Catalytic Alumina,-No Promoter														
17		0.15	0.17	0.24	0.50	0.88	0.83	266	7.7	34.8	65.5	77.9	88.0	91.9		54.5	2.35	27.7	62.0	86.7	94.0	98.7		
												Reforming Catalyst						23.6	50.9	70.0	86.2	95.5		
18	Pt-Al_2O_3Cl	0.17	0.20	0.33	0.59	0.54	0.47	178	5.2	22.3	41.0	63.3	79.8	90.9		42.0	2.03	10.4	37.2	78.0	95.8			
19	Pt-Al_2O_3Cl	0.16	0.18	0.29	0.71	0.56	0.55	179	2.6	21.8	67.8	95.7				53.0	1.56	28.0	67.0	83.5	92.5	95.6		
20	Pt-Al_2O_3Cl	0.21	0.25	0.39	0.78	0.56	0.55	252	11.6	43.2	61.7	74.7	87.3	92.0		40.0	2.00	13.8	44.6	70.2	84.0	96.4		
21	Pt-Al_2O_3Cl	0.17	0.21	0.36	0.65	0.56	0.55	196	3.2	23.7	50.4	70.3	93.4			46.0	2.03	33.3	52.5	77.7	90.9	96.6		
22	Pt-Al_2O_3-Cl	0.15	0.18	0.28	0.56	0.60	0.55	183	8.3	21.9	49.9	70.5	81.7	93.1		46.0	1.97	6.9	28.9	81.5	98.2			
23	Pt-Al_2O_3-Cl	0.16	0.19	0.28	0.78	0.61	0.61	196	1.7	17.4	76.6					46.0	1.39	11.3	30.4	63.1	12.1			
24	Pt-Al_2O_3-Cl	0.20	0.22	0.34	0.74	0.54	0.53	211	2.4	15.0	43.9	80.9	99.5			44.0	1.61	1.5	9.1	68.5	91.8			
25	Pt-Al_2O_3-Cl	0.21	0.24	0.37	0.93	0.55	0.55	233	0.3	4.1	55.8	83.9	96.2			46.0	1.45	8.5	29.3	79.0	62.4			
26	Pt-Al_2O_3-Cl	0.17	0.20	0.30	0.77	0.60	0.60	210	2.0	16.0	68.2	93.4				52.0	1.45	4.6	21.0	74.8	93.0			
27	Pt-Al_2O_3-Cl	0.21	0.22	0.34	0.84	0.52	0.52	206	0.0	10.6	60.3	83.5	97.2			48.0	1.47	19.5	49.7	87.3	95.4			
28	Pt-Al_2O_3-Cl	0.14	0.16	0.26	0.60	0.54	0.52	158	5.5	29.6	71.6	92.7				56.0	1.73	47.1	62.5	75.2	87.2	94.9	99.1	
29	Pt-Al_2O_3-Cl	0.15	0.17	0.27	0.46	0.49	0.41	147	13.0	25.1	40.7	61.4	78.3	89.9	95.9	41.5	2.31	48.1	90.9	97.4	99.4			
30	Pt-Al_2O_3Cl	0.09	0.10	0.14	0.25	0.94	0.85	176	20.9	74.0	86.2	91.1	95.2			1 03.0	1.82	30.3	37.8	49.8	58.7	66.2	73.0	79.1
31	Pt-Al_2O_3-Cl	0.37	0.42	0.52	0.67	0.56	0.49	412	3.4	5.7	11.7	17.8	24.5	32.1	39.9	15.0	3.36							

[a] Based on adsorption.
[b] Values in these lines based on desorption.

Restrictions 2c and 2d are imposed in order that P_{50} and P_{25}/P_{75} will in fact have physically correct dimensions (Angstroms and dimensionless, respectively). The results of the least squares fitting of Model 2 to the data are given in Table II.

The similarity of 2a to known formulas for locating pore size distributions is apparent. Indeed, as shown in 3a to 3c, fitting of 2a to all data either with or without Restriction 2c and fitting Wheeler's model directly all give similar results

$$\text{Unrestricted} \quad P_{50} = 1.52 \times 10^{-4} V^{1.03} A^{-0.86} \tag{3a}$$

$$\text{Restricted} \quad P_{50} = 1.74 \times 10^{-4} V^{0.92} A^{-0.88} \tag{3b}$$

$$\text{Ratio only} \quad P_{50} = 1.73 \times 10^{-4} V/A$$

One way of considering the type of prediction available is shown in Figures 3 and 4. From the distributions calculated from Model 2, the percentiles of the distributions corresponding to a mean pore wall separation of 20 A. are predicted for the mixed gel type (cracking catalyst) (Figure 3). Similarly, at 40 A. the percentiles are predicted for the more coarsely structured alumina-based materials (Figure 4). Within these two groups, the use of the model gives some predictability of the area associated with pores of a possibly kinetically significant size.

Table II. Fitting of Model 2 to Data of Table I

$Y_1 = \log_{10} P_{50}$		$X_1 = \log_{10}(10\ V)$	
$Y_2 = \log_{10} P_{75}/P_{25}$		$X_2 = \log_{10}(A/100)$	
a_0	1.242	b_0	0.333
a_1	0.918	b_1	−0.145
a_2	−0.877	b_2	0.217
RMS error (Y_1) = 17%		RMS error (Y_2) = 27%	

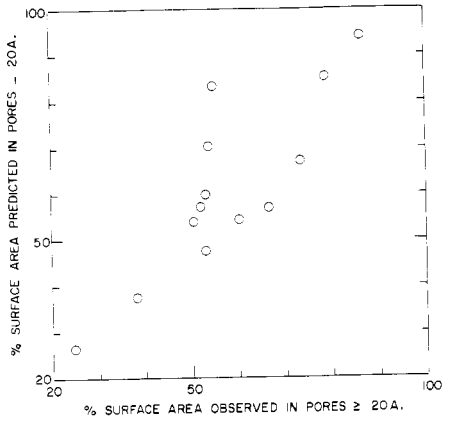

Figure 3. Prediction of percentiles corresponding to 20-A. pores in cracking catalysts

Various attempts to improve the prediction by including also the nitrogen pore volume or the value of the isotherm at $p/p_0 = 0.5$ did not appear to lead to improved estimation of the observed distributions.

In cases where continued work with a particular type of material is desired, it might be considered worthwhile to develop a correlation like 2 specifically for the material of interest.

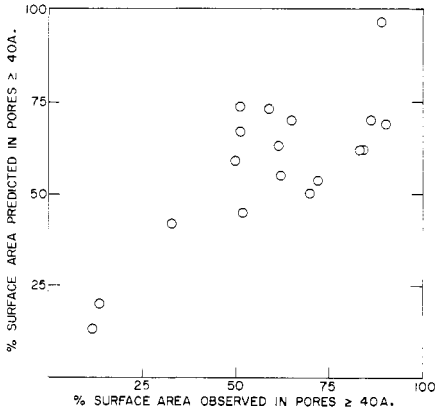

Figure 4. Prediction of percentiles corresponding to 40-A. pores in alumina-based materials

LITERATURE CITED

(1) American Cyanamid Co., Refinery Chemicals Department, New York, N. Y., "Test Methods for Synthetic Fluid Cracking Catalyst."
(2) Ashley, K.D., Innes, W.B., *Ind. Eng. Chem.* **44**, 2857 (1952).
(3) Barrer, R.M., Gabor, T., *Proc. Roy. Soc. (London)* **A251**, 353 (1959).
(4) Barrett, E.P., Joyner, L.G., Halenda, P.P., *J. Am. Chem. Soc.* **60**, 373 (1951).
(5) Brunauer, S., Emmett, P.H., Teller, E., *Ibid.*, **60**, 309 (1938).
(6) Cranston, R.W., Inkley, F.W., *Advances in Catalysis* **9**, 143 (1959).
(7) Derjaguin, B.V., *Doklady Akad. Nauk S.S.S.R.* **113**, 842 (1957).
(8) Everett, D.H., Stone, F.S., eds., "Structure and Properties of Porous Materials," Academic Press, New York, 1958.
(9) Innes, W.B., *Anal. Chem.* **23**, 759 (1951).
(10) *Ibid.*, **28**, 332 (1956).
(11) *Ibid.*, **29**, 1069 (1957).
(12) Ritter, H.L., Drake, L.C., *Ind. Eng. Chem., Anal. Ed.* **17**, 787 (1945).
(13) Steggerda, J., "De Vorming van Actief Aluminiumoxide," Delft, Holland, 1955.
(14) Wheeler, A., in "Catalysis," P.H. Emmett, ed., vol. **2**, p. 105, Reinhold, New York, 1955.

RECEIVED for review November 23, 1960. Accepted July 24, 1961.